Neurotoxicology 67 (2018) 215–225

Contents lists available at ScienceDirect

Neurotoxicology

journal homepage: www.elsevier.com/locate/neuro

# Human iPSC-derived neuronal models for *in vitro* neurotoxicity assessment

Anke M. Tukker, Fiona M.J. Wijnolts, Aart de Groot, Remco H.S. Westerink*

*Neurotoxicology Research Group, Toxicology and Pharmacology Division, Institute for Risk Assessment Sciences (IRAS), Faculty of Veterinary Medicine, Utrecht University, P.O. Box 80.177, NL-3508 TD, Utrecht, The Netherlands*

ARTICLE INFO

*Keywords:*
*In vitro* neurotoxicity screening
Human induced pluripotent stem cell-derived neuronal models
Micro-Electrode array (MEA)
Alternatives to animal testing
Mixed neuronal cultures
Astrocytes

ABSTRACT

Neurotoxicity testing still relies on ethically debated, expensive and time consuming *in vivo* experiments, which are unsuitable for high-throughput toxicity screening. There is thus a clear need for a rapid *in vitro* screening strategy that is preferably based on human-derived neurons to circumvent interspecies translation. Recent availability of commercially obtainable human induced pluripotent stem cell (hiPSC)-derived neurons and astrocytes holds great promise in assisting the transition from the current standard of rat primary cortical cultures to an animal-free alternative.

We therefore composed several hiPSC-derived neuronal models with different ratios of excitatory and inhibitory neurons in the presence or absence of astrocytes. Using immunofluorescent stainings and multi-well micro-electrode array (mwMEA) recordings we demonstrate that these models form functional neuronal networks that become spontaneously active. The differences in development of spontaneous neuronal activity and bursting behavior as well as spiking patterns between our models confirm the importance of the presence of astrocytes. Preliminary neurotoxicity assessment demonstrates that these cultures can be modulated with known seizurogenic compounds, such as picrotoxin (PTX) and endosulfan, and the neurotoxicant methylmercury (MeHg). However, the chemical-induced effects on different parameters for neuronal activity, such as mean spike rate (MSR) and mean burst rate (MBR), may depend on the ratio of inhibitory and excitatory neurons. Our results thus indicate that hiPSC-derived neuronal models must be carefully designed and characterized prior to large-scale use in neurotoxicity screening.

## 1. Introduction

Human induced pluripotent stem cell (hiPSC)-derived neuronal cultures are becoming increasingly important for *in vitro* neurotoxicity testing. These neuronal cultures could provide an alternative for costly, time consuming and ethically debated animal experiments or *in vitro* work with primary cultures. Moreover, there is a clear need for alternatives of human origin since animal-based models do not always mimic the human physiology and can therefore in some cases be poor predictors for human adverse outcomes (Hartung, 2008).

The use of hiPSC-derived neurons for neurotoxicity testing would circumvent the need for interspecies translation. As such, the recent commercial availability of these neuronal models holds great promise in assisting the transition from the current gold standard of rat primary cortical cultures (Alloisio et al., 2015; Dingemans et al., 2016; Hogberg et al., 2011; Hondebrink et al., 2016; McConnell et al., 2012; Nicolas et al., 2014; Valdivia et al., 2014; Vassallo et al., 2017) to hiPSC-derived models (Tukker et al., 2016). We have recently shown that these commercially available models have the potential to develop spontaneously active neuronal networks that can be used for screening and prioritization of chemically induced effects on neuronal activity (Tukker et al., 2016), whereas others have already shown that hiPSC-derived neurons exhibit the behavior and function of mature neurons (Hyysalo et al., 2017; Odawara et al., 2016; Paavilainen et al., 2018). While costly in comparison to (rodent) primary cultures and (human) neural progenitor cells, an important benefit of hiPSC-derived neurons is the rapid development of a functional neuronal network, in contrast to the time consuming differentiation of hiPSCs into neural progenitor cells that subsequently need to be cultured into functional neurons, a process that can take several weeks (Görtz et al., 2004; Hyysalo et al., 2017; Kuijlaars et al., 2016) till months (Odawara et al., 2016; Paavilainen et al., 2018). Opting for these commercially obtainable cells comes with the additional benefit that they are available in high quantity, allowing for efficient screening (Anson et al., 2011). On the other hand, besides being costly, hiPSC-derived neurons have the disadvantage of being less well characterized for electrophysiological studies and have so far been little used for neurotoxicity screening.

*In vitro* screening models should represent the *in vivo* situation as

* Corresponding author.
*E-mail address:* R.Westerink@uu.nl (R.H.S. Westerink).

https://doi.org/10.1016/j.neuro.2018.06.007
Received 30 November 2017; Received in revised form 24 April 2018; Accepted 12 June 2018

**Table 1**
Composition and density of the different cell models.

| Type of culture | Cell types and ratio | Seeding density/ well or chamber |
|---|---|---|
| iCell® Glutaneuron monoculture | 100% Glutaneurons | 80,000 |
| iCell® Glutaneuron-iCell® neuron co-culture | 20% iCell neurons<br>80% Glutaneurons | 80,000 |
| iCell® Glutaneuron-iCell®-Astrocyte co-culture | 50% Glutaneurons<br>50% Astrocytes | 150,000 |
| iCell® Glutaneuron-iCell® neuron-iCell® Astrocyte co-culture | 40% Glutaneurons<br>10% iCell neurons<br>50% Astrocytes | 140,000 |

closely as possible and must contain sufficient complexity to answer the research question (Pamies and Hartung, 2017; Westerink, 2013). With regard to neurotoxicity testing, this means that the model must capture the complexity and diversity of cell types of the human brain. It thus must form functional networks with a controlled balance of excitatory and inhibitory neurons as well as supportive cells. However, until now, most studies focused on cell cultures containing only hiPSC-derived neurons, whereas other neuronal cell types and/or astrocytes should also be included. Astrocytes, for example, play an important role in the regulation of the development of neurons (Tang et al., 2013) and also have been shown to enhance the development of neuronal networks and action potentials in human iPSC-derived co-cultures (Ishii et al., 2017). The addition of astrocytes to the neuronal model has also been reported to increase synchrony of the networks (Amiri et al., 2013). Moreover, inclusion of astrocytes also adds specific, physiologically relevant targets for toxic insults to the culture that would not be present in a pure neuronal model. Notably in this respect, there is growing evidence that astrocytes can play a protective role against chemical-induced neurotoxicity (Takemoto et al., 2015; Wu et al., 2017).

Currently, however, there is still a knowledge gap that has to be filled before co-cultured hiPSC-derived models can replace the primary rat cortical cultures and become the new gold standard for mwMEA experiments. For example, the role of different cell types in hiPSC-derived neuronal cultures is largely unexplored and concerns regarding the immature phenotype, including limited bursting, have been raised (Meneghello et al., 2015). We therefore composed different (co-)cultures of iCell Glutaneurons® (~90% excitatory glutamatergic neurons/ 10% inhibitory GABAergic neurons) and iCell neurons® (~30% excitatory glutamatergic neurons/70% inhibitory GABAergic neurons) in the absence or presence of astrocytes to explore the role of different cell types in development of neuronal activity and suitability for *in vitro* neurotoxicity testing, including seizure liability testing.

## 2. Materials and methods

### 2.1. Chemicals

N2 supplement, penicillin-streptomycin (10.000 U/mL–10.000 µg/mL), Geltrex, phosphate-buffered saline (PBS), fetal bovine serum (FBS), DMEM, trypsin-EDTA, 4′,6-diamidino-2-phenylindole (DAPI), donkey anti-rabbit Alexa Fluor® 488 and donkey anti-mouse Alexa Fluor® 594 were obtained from Life Technologies (Bleiswijk, The Netherlands). FluorSave was obtained from Calbiochem (San Diego, California, USA). iCell® Neurons Maintenance medium, iCell® Neurons Medium Supplement and Nervous System Supplement were obtained from Cellular Dynamics International (Madison, WI, USA). Rabbit anti-β(III)-tubulin (Ab18207), mouse anti-S100β (Ab11178) and rabbit anti-vGluT1 (Ab104898) were obtained from Abcam (Cambridge, United Kingdom). Mouse anti-vGAT (131001) was obtained from Synaptic Systems (Göttingen, Germany). BrainPhys neuronal medium was obtained from StemCell Technologies (Cologne, Germany). Paraformaldehyde (PFA) was obtained from Electron Microscopy Sciences (Hatfield, Pennsylvania, USA). Picrotoxin (PTX), endosulfan (α:β 2:1 99.9%), methylmercury (MeHg), 50% polyethyleneimine (PEI) solution, laminin, sodium borate, boric acid, bovine serum albumin and all other chemicals (unless described otherwise) were obtained from Sigma-Aldrich (Zwijndrecht, The Netherlands).

Stock solutions of endosulfan and MeHg were prepared in dimethyl sulfoxide (DMSO). For PTX, stock solutions were freshly prepared in ethanol (EtOH) directly before every experiment.

**Table 2**
Overview and description of used metric parameters.

| Metric parameter | Description |
|---|---|
| Mean spike rate (MSR) | Total number of spikes divided by recording time (Hz) |
| ISI coefficient of variation | Standard deviation ISI (time between spikes) divided by the mean ISI. Measure for spike regularity: 0 indicates perfect spike distribution, > 1 signals bursting |
| Burst duration | Average time from the first spike in a burst till the last spike (s) |
| Number of spikes per burst | Average number of spikes occurring in a burst |
| Mean ISI within burst | Mean inter-spike interval within a burst (s) |
| Median ISI within burst | Median inter-spike interval within a burst (s) |
| Inter-burst interval (IBI) | Time between the last spike of a burst and the first spike of a subsequent burst (s) |
| Burst frequency | Total number of bursts divided by recording time (Hz) |
| IBI coefficient of variation | Standard deviation of IBI divided by the mean IBI. Measure for burst regularity |
| Burst percentage | Percentage of total number of spikes occurring in a burst |
| Network burst frequency | Total number of network bursts divided by recording time (Hz) |
| Network burst duration | Average time from the first spike till the last spike in a network burst (s) |
| Number of spikes per network burst | Average number of spikes occurring in a network burst |
| Mean ISI within network burst | Average of the mean ISIs within a network burst (s) |
| Median ISI within network burst | Average of the median ISIs within a network burst (s) |
| Number of spikes per network burst/channel | Average number of spikes in a network burst divided by the electrodes participating in that burst |
| Network burst percentage | Percentage of total spikes occurring in a network burst |
| Network IBI coefficient of variation | Standard deviation of network IBI divided by the mean network IBI. Measure of network burst rhythmicity: value is small when bursts occur at regular interval and increases when bursts occur more sporadic |
| Network normalized duration IQR | Interquartile range of network bursts durations. Measure for network burst duration regularity: larger values indicate wide variation in duration. |
| Area under normalized cross-correlation | Area under inter-electrode cross-correlation normalized to the auto-correlations. The higher the value, the greater the synchronicity of the network. |
| Full width at half height of normalized cross-correlation | Width at half height of the normalized cross-correlogram. Measure for network synchrony: the higher the value, the less synchronised the network is. |

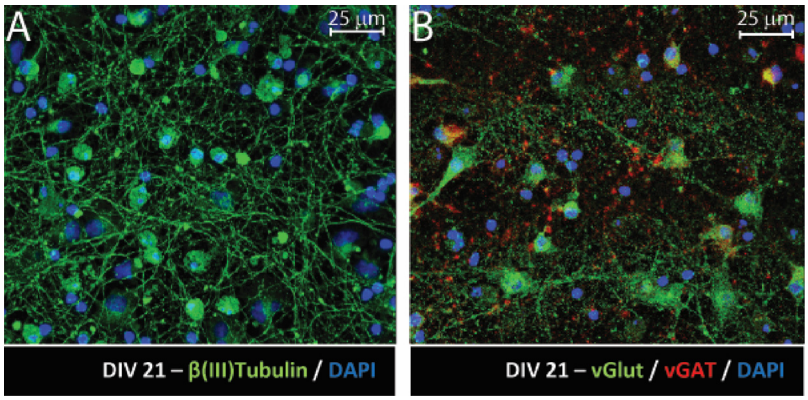


**Fig. 1.** Immunofluorescent stainings of the iCell® Glutaneuron monoculture (A) and iCell® Glutaneuron-iCell® neuron co-culture (B). At DIV21 the monoculture was stained with β(III)tubulin (green) to identify neurons and show network formation (A). To demonstrate the presence of GABAergic and glutamatergic neurons in the iCell® Glutaneuron-iCell® neuron co-culture cells were stained with vGAT (red) and vGlut (green) (B). Nuclei are stained with DAPI (blue). Scale bar depicts 25 µm. (For interpretation of the references to colour in this figure legend, the reader is referred to the web version of this article).

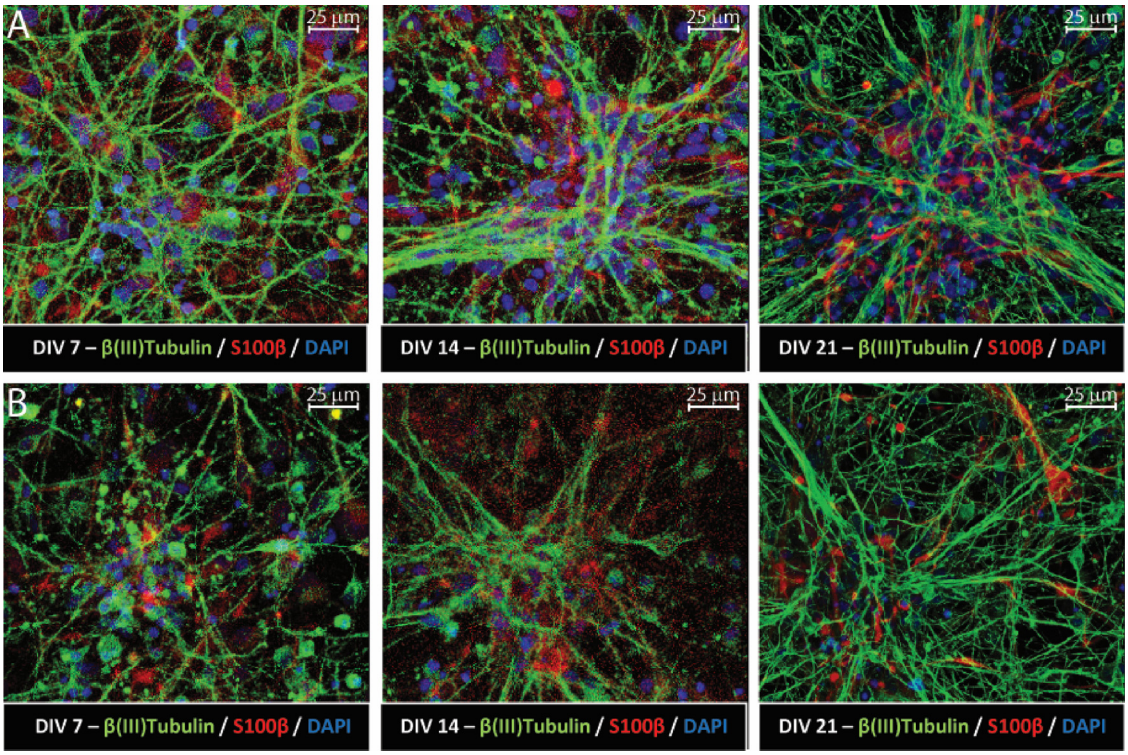


**Fig. 2.** Immunofluorescent stainings of the different hiPSC-derived neuronal co-cultures with astrocytes. At DIV7 (left), 14 (middle) and 21 (right) cultures were stained with β(III)tubulin (green) and S100β (red) to identify respectively neurons and astrocytes in the iCell® Glutaneuron-Astrocyte co-culture (A) and iCell® Glutaneuron-iCell® neuron-Astrocyte co-culture (B). Nuclei are stained with DAPI (blue). Scale bar depicts 25 µm. (For interpretation of the references to colour in this figure legend, the reader is referred to the web version of this article).

### 2.2. Cell culture

Cells were cultured at 37 °C in a humidified 5% $CO_2$ incubator in line with supplier's instructions. All cell culture surfaces (coverslips and MEA plates) were pre-coated with 0.1% PEI solution diluted in borate buffer (24 mM sodium borate/50 mM boric acid in Milli-Q adjusted to pH 8.4) unless stated otherwise.

iCell® Astrocytes (Cellular Dynamics International, Madison, WI, USA) were thawed and cultured in DMEM with high glucose and 10% FBS, 1% N2 supplement and 1% penicillin-streptomycin, and were grown for 3–4 passages in Geltrex-coated culture flasks before using them in the co-cultures. Culture medium was refreshed every 3–4 days.

iCell® Glutaneurons and iCell® Neurons (Cellular Dynamics International, Madison, WI, USA) were thawed in Complete iCell Neurons Maintenance Medium supplemented with 2% iCell Neurons medium supplement, 1% penicillin-streptomycin and 1% laminin (10 µg/mL).

Before final plating, cells were pre-mixed into one of the four desired cultures: 1) monoculture of iCell® Glutaneurons, 2) co-culture of iCell® Glutaneurons and iCell® neurons, 3) co-culture of iCell® Glutaneurons and iCell® Astrocytes and 4) co-culture of iCell® Glutaneurons, iCell® neurons and iCell® Astrocytes. The different cell culture models and total number of cells/well or cells/chamber are described in Table 1.

For immunofluorescent stainings, the different cell culture models were seeded on 8-chamber coverslips (Ibidi GmbH, Planegg, Germany) in 10 µL droplets of cell suspension with a density of 80,000 cells/droplet for the iCell® Glutaneuron monoculture and iCell® Glutaneuron-iCell® neuron co-culture; 150,000 cells/droplet for the iCell® Glutaneuron-iCell® Astrocyte co-culture and 140,000 cells/droplet for the iCell® Glutaneuron-iCell® neuron-iCell® Astrocyte co-culture. For multi-well micro-electrode array (mwMEA) experiments, cells were seeded as 10 µL droplets of cell suspension, with the same seeding density/droplet as described above, directly over the electrode field of

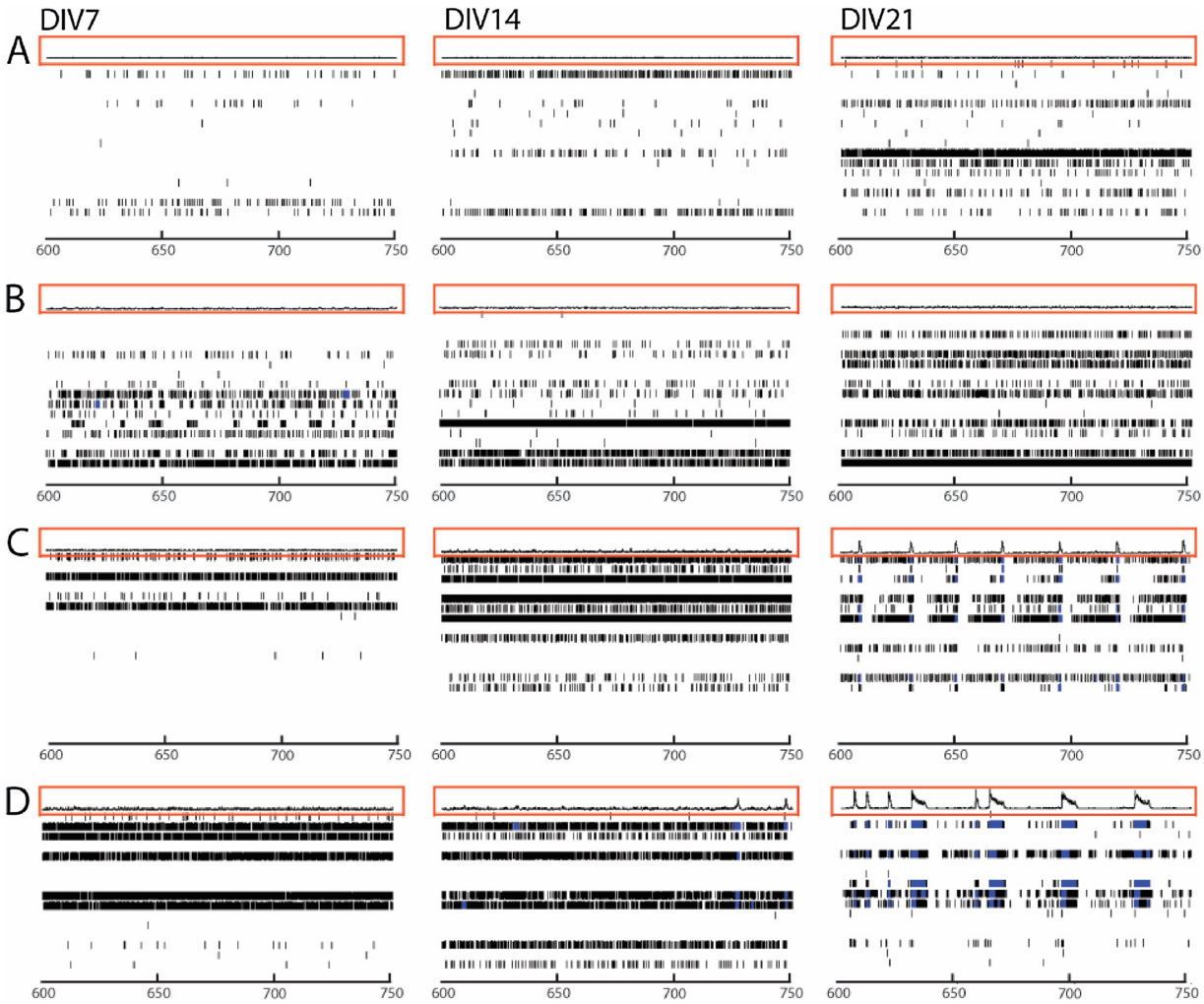


**Fig. 3.** Spike raster plots of different hiPSC-derived cultures. Each row depicts one electrode in a representative example well, with each tick representing one spike (field potential) in a 150 s interval. This illustrates the degree and pattern of activity of the iCell® Glutaneuron monoculture (A), the iCell® Glutaneuron-iCell® neuron co-culture (B), the iCell® Glutaneuron-Astrocyte co-culture (C) and the iCell® Glutaneuron-iCell® neuron-Astrocyte co-culture (D) at DIV7 (left), DIV14 (middle) and DIV21 (right). The cumulative trace in the orange box above each raster plot depicts the population spike time histogram indicating the synchronized activity between the different electrodes (network burst). (For interpretation of the references to colour in this figure legend, the reader is referred to the web version of this article).

each well of a 48-well MEA plate (Axion Biosystems Inc., Atlanta, GA, USA). The droplets of cell suspension, both on the coverslips and on the MEA plates, were allowed to adhere for 1 h in a humidified incubator at 37 °C and 5% $CO_2$. Next, room temperature (RT) supplemented BrainPhys medium (BrainPhys neuronal medium supplemented with 2% iCell Neuron supplement, 1% Nervous System supplement, 1% penicillin-streptomycin, 1% N2 supplement and 0.1% laminin (10 µg/mL)) was added (300 µL for MEA, 200 µL for chambers), and cells were placed back in the humidified incubator. After 1 day *in vitro* (DIV1), 50% of the medium was refreshed with RT supplemented BrainPhys medium. Hereafter, 50% medium changes took place 3 times a week up till DIV21.

### 2.3. Immunocytochemistry

The different hiPSC-derived neuronal (co-)cultures were fixated as described previously (Tukker et al., 2016) on DIV7, 14 and 21 with 4% PFA in 0.1 M PBS (pH 7.4) for 15 min at RT. Briefly, following fixation coverslips were quenched for PFA, permeabilized and incubated for 20 min at RT with 20 mM $NH_4Cl$ in blocking buffer (2% bovine serum albumin and 0.1% saponin in PBS). Next, coverslips were incubated overnight at 4 °C with rabbit anti-βIII tubulin (final dilution 1:250), mouse anti-S100β (final dilution 1:500), mouse anti-vGAT (final dilution 1:1000) and/or rabbit anti-vGluT1 (final dilution 1:1500) in blocking buffer. Hereafter, coverslips were washed 3 times with blocking buffer and incubated with donkey anti-mouse Alexa Fluor® 488 and/or donkey anti-rabbit Alexa Fluor® 594 (final dilution 1:100) for 30 min at RT in the dark. Coverslips were incubated for 2–3 min with 200 nM DAPI at RT in the dark for nuclear staining. Coverslips were again washed 3 times with blocking buffer and sealed with FluorSave. The coverslips were stored at 4 °C in the dark until further use. Immunostained coverslips were visualized with a Leica SPEII Confocal microscope (Leica DMI4000 equipped with TCS-SPE-II) using a 20x oil immersion objective (N.A. 1.4-0.7). Images were captured as. tiff files using Leica Application Suite Advanced Fluorescence software (LAS AF version 2.6.0; Leica Microsystems GmbH, Wetzlar, Germany).

### 2.4. MEA measurements

The different hiPSC-derived neuronal (co-)cultures were cultured on 48-well PEI-coated MEA plates (Axion Biosystems Inc., Atlanta, GA, USA). Each well contains an electrode array of 16 nanotextured gold micro-electrodes (40–50 µm diameter; 350 µm center-to-center spacing) with 4 integrated ground electrodes, yielding a total of 768 channels,

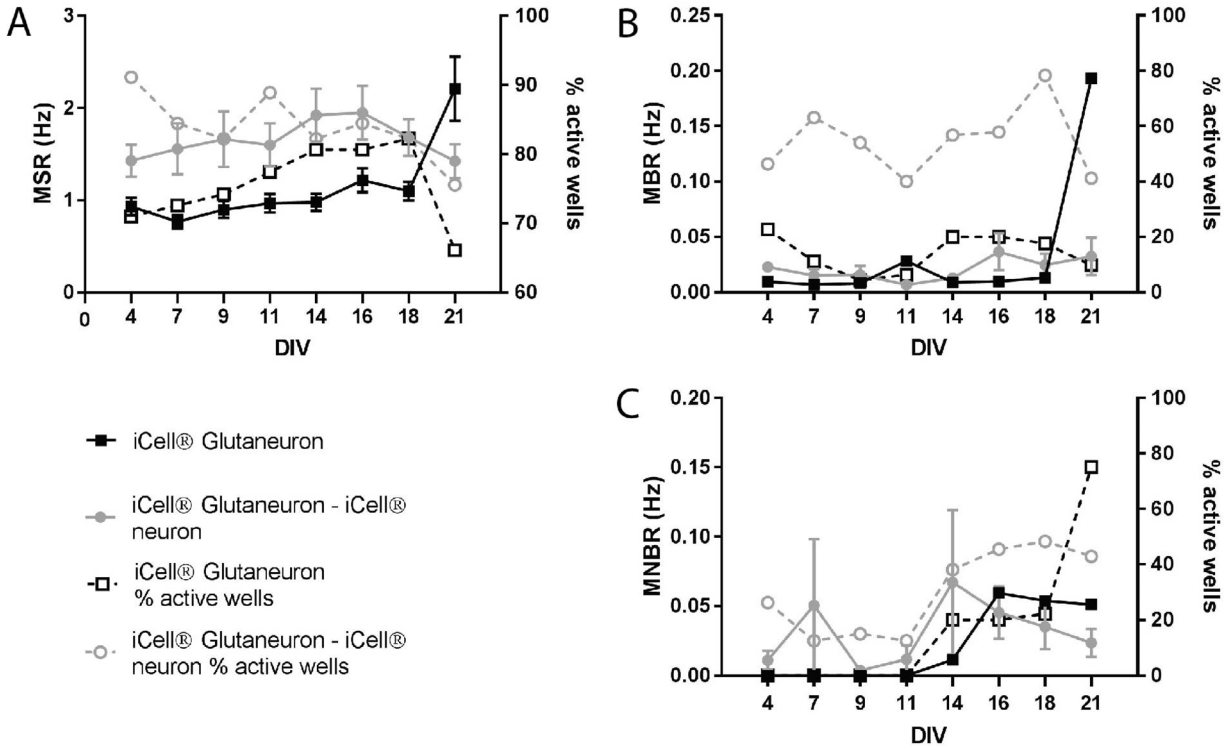


**Fig. 4.** Development of spontaneous neuronal activity and (network) bursting in different h-iPSC-derived neuronal (co-)cultures. A) Mean spike rate (MSR (Hz); solid lines) and percentage of spiking wells (dashed lines) are depicted in for the iCell® Glutaneuron monoculture (black lines; n = 41–51, N = 3) and iCell® Glutaneuron-iCell® neuron co-culture (grey lines; n = 34–41, N = 4). B) Mean burst rate (MBR (Hz); solid lines) and percentage of bursting wells (dashed lines) are depicted for the iCell® Glutaneuron monoculture (black lines; n = 2–10, N = 3) and iCell® Glutaneuron-iCell® neuron co-culture (grey lines; n = 14–29, N = 4). C) Mean network burst rate (MNBR (Hz); solid lines) and percentage of network bursting wells (dashed lines) are depicted for the iCell® Glutaneuron monoculture (black lines; n = 2–3, N = 3) and iCell® Glutaneuron-iCell® neuron co-culture (grey lines; n = 2–14, N = 4). Data are expressed as mean ± SEM from n wells and N cultures.

which can be recorded at the same time. Spontaneous network activity was recorded at 37 °C without further climate control at DIV4, 7, 9, 11, 14, 16, 18 and 21 as described previously (de Groot et al., 2014; Dingemans et al., 2016). Briefly, signals were recorded using a Maestro 768-channel amplifier with integrated heating system and temperature controller and a data acquisition interface (Axion Biosystems Inc., Atlanta, GA, USA). Data acquisition was managed with Axion's Integrated Studio (AxIS version 2.4.2.13). MEA plates were allowed to equilibrate for ~5 min prior to the 30 min recording of spontaneous activity. Raw data files were obtained by sampling the channels simultaneously with a gain of 1200x and a sampling frequency of 12.5 kHz/channel using a band-pass filter (200–5000 Hz).

To determine effects of test compounds on spontaneous activity (spiking and bursting behavior) of the different hiPSC (co-)cultures, activity was recorded at DIV21. Immediately after this baseline recording, wells were exposed (dilution 1:10) to test compounds or the appropriate solvent control (DMSO or EtOH) and activity was recorded for another 30 min. Stock solutions of endosulfan, MeHg and PTX were diluted in supplemented BrainPhys culture medium to obtain the desired concentrations. In all experiments the solvent concentration never exceeded 0.1% v/v.

### 2.5. Data analysis and statistics

After recording spontaneous activity, raw files were re-recorded to obtain Alpha Map files for further data analysis. During the re-recording, spikes were detected using the AxIS spike detector (Adaptive threshold crossing, Ada BandFIt v2) with a variable threshold spike detector set at 7x standard deviation (SD) of internal noise level (rms) on each electrode. The resulting spike count files were loaded into NeuroExplorer 5.020 software (Nex Technologies, Madison, Wisconsin) for further analysis. For all experiments, spike files were loaded in Neural Metric (version 2.04, Axion Biosystems). Only active electrodes (MSR ≥ 6 spikes/min) in active wells (≥1 active electrode) were included in the analysis. Mean burst rate (MBR) was extracted with the Poisson Surprise method with a minimal surprise of 10 (Legéndy and Salcman, 1985) and a minimum bursting frequency of 0.001 bursts/sec. Network bursts were extracted using the adaptive threshold method.

For constructing developmental curves, the full 30 min recordings obtained at DIV4, 7, 9, 11, 14, 16, 18 and 21 were used for data analysis. Neural metric outputs were loaded in a custom-made Excel macro to select only those electrodes that fit the activity criteria. Only wells with a minimum of 2 bursting electrodes were used to calculate network and synchronicity parameters. Percentages of spiking wells were calculated compared to the number of plated wells, percentages of bursting wells were calculated compared to the number of spiking wells, and percentages of network bursting wells were calculated compared to the number of bursting wells.

The effects of test compounds were determined in exposure experiments at DIV21 in which the baseline activity prior to exposure was compared to activity following exposure. To prevent inclusion of artifacts, a correction for the time it took to expose the wells was performed. For example, if it took 3 min to expose the mwMEA plate, the first 3 min of the recording were not used for data analysis, only the subsequent 30 min.

For exposure experiments, a custom-made excel macro was used to establish treatment ratios per well for the different metric parameters (Table 2) by expressing the $parameter_{exposure}$ as a percentage change compared to the $parameter_{baseline}$. Only those electrodes in a well that fit the activity criteria during baseline recording were used to calculate well averages. All electrodes defined as active in baseline recordings were then used to calculate well averages during exposure. Next,

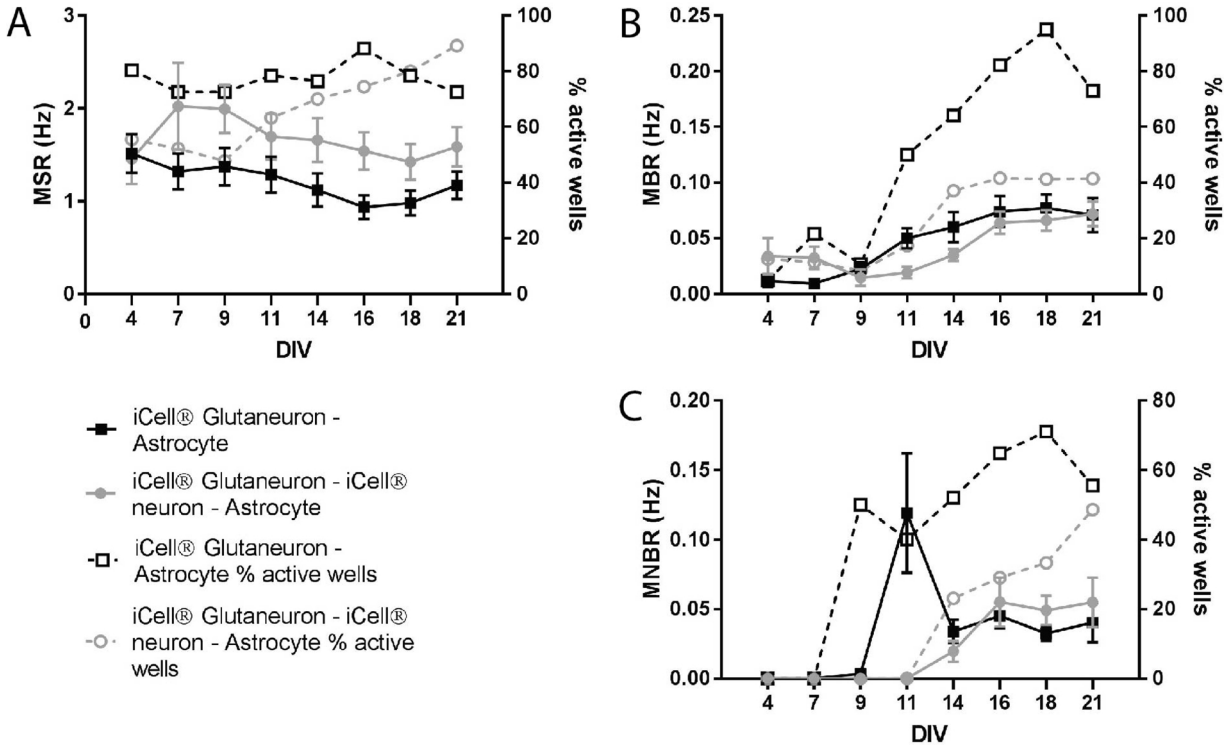


**Fig. 5.** Development of spontaneous neuronal activity and (network) bursting in different hiPSC-derived neuronal co-cultures with astrocytes. A) Mean spike rate (MSR (Hz); solid lines) and percentage of spiking wells (dashed lines) are depicted for the iCell® Glutaneuron-Astrocyte co-culture (black lines; n = 43–72, N = 4) and iCell® Glutaneuron-iCell® neuron-Astrocyte co-culture (grey lines; n = 34–41, N = 4). B) Mean burst rate (MBR (Hz); solid lines) and percentage of bursting wells (dashed lines) are depicted for the iCell® Glutaneuron-Astrocyte co-culture (black lines; n = 2–38, N = 4) and iCell® Glutaneuron-iCell® neuron-Astrocyte co-culture (grey lines; n = 4–37, N = 5). C) Mean network burst rate (MNBR (Hz); solid lines) and percentage of network bursting wells (dashed lines) are depicted for the iCell® Glutaneuron-Astrocyte co-culture (black lines; n = 2–27, N = 4) and iCell® Glutaneuron-iCell® neuron-Astrocyte co-culture (grey lines; n = 6–18, N = 5). Data are expressed as mean ± SEM from n wells and N cultures.

treatment ratios were normalized to the appropriate vehicle control. Outliers in control and effect data (defined as not within average ± 2 x SD) were excluded from further data analysis (2%). All data are presented as mean ± SEM from the number of wells (*n*, with a minimum of 2 wells). SEM is used as statistical measure as it reflects the accuracy of the reported value with respect to the "true mean" of the population assessed, rather than providing a descriptive measure that reflects the variability within the population such as the SD (Pleil, 2016), and for easy comparability with published datasets (*e.g.* Alloisio et al., 2015; Brown et al., 2016; Dingemans et al., 2016; Hogberg et al., 2011; Strickland et al., 2016). A *t*-test was performed to determine significant changes ($p < 0.05$) in MSR or MBR compared to the vehicle control.

## 3. Results

### 3.1. Immunofluorescent stainings of the different human iPSC-derived neuronal models

As a first characterization, the iCell® Glutaneuron monoculture was cultured for up to 3 weeks and labelled with β(III)tubulin antibodies at DIV21 to identify the presence of neurons and to visualize network formation (Fig. 1A). To discriminate between subtypes of neurons in the iCell® Glutaneuron-iCell® neuron co-culture, vesicular transporters of glutamate (vGlut) and GABA (vGAT) were stained (Fig. 1B). This co-culture shows a clear expression of vGlut and vGAT indicating the co-existence of respectively excitatory and inhibitory neurons. Both cultures show a pure neuronal phenotype. The heterogeneity of the culture can be increased by co-culturing the neurons with astrocytes.

Co-cultures containing astrocytes were also cultured up to 3 weeks and were labelled with S100β and β(III)tubulin antibodies at DIV7, 14 and 21 to identify the presence of respectively astrocytes and neurons (Fig. 2A and B). Both models show network formation with a high degree of complexity. Network density and complexity increases with prolonged culture duration. In both models, neurons and astrocytes distribute evenly to form mixed networks. Visual observation indicates that the ratio astrocyte to neuron is stable during the entire culture duration.

These results show that the different hiPSC-derived (co-)cultures all consist of inhibitory GABAergic and excitatory glutamatergic neurons and, when added, supporting astrocytes. The data also indicate that neuronal networks are formed, suggesting that they could be suitable for neurotoxicity screening.

### 3.2. Development of spontaneous electrical activity and bursting

In order to further test the applicability of our different hiPSC-derived neuronal models for neurotoxicity screening, cells were cultured for up to 21 days on mwMEAs. Development of spontaneous neuronal network activity and bursting behavior over time were assessed. The spontaneous electrical activity at DIV7, 14 and 21 is depicted in spike raster plots (Fig. 3). The plots show that all models develop spontaneous neuronal activity, although the pattern of activity differs strongly between the models. Models without astrocytes (Fig. 3A and B) do not show synchronicity, whereas models with astrocytes synchronize their activity with prolonged culture duration (Fig. 3C and D). All tested models develop bursting, but the amount of bursts differs per culture. The iCell® Glutaneuron monoculture and iCell® Glutaneuron-iCell® neuron co-culture show few bursting electrodes (Fig. 3A and B), in contrast to the co-cultures containing astrocytes where almost all active electrodes show bursting (Fig. 3C and D).

In all tested cultures the mean spike rate (MSR) is relatively stable over time (Figs. 4A and 5A). Addition of the more inhibitory iCell®

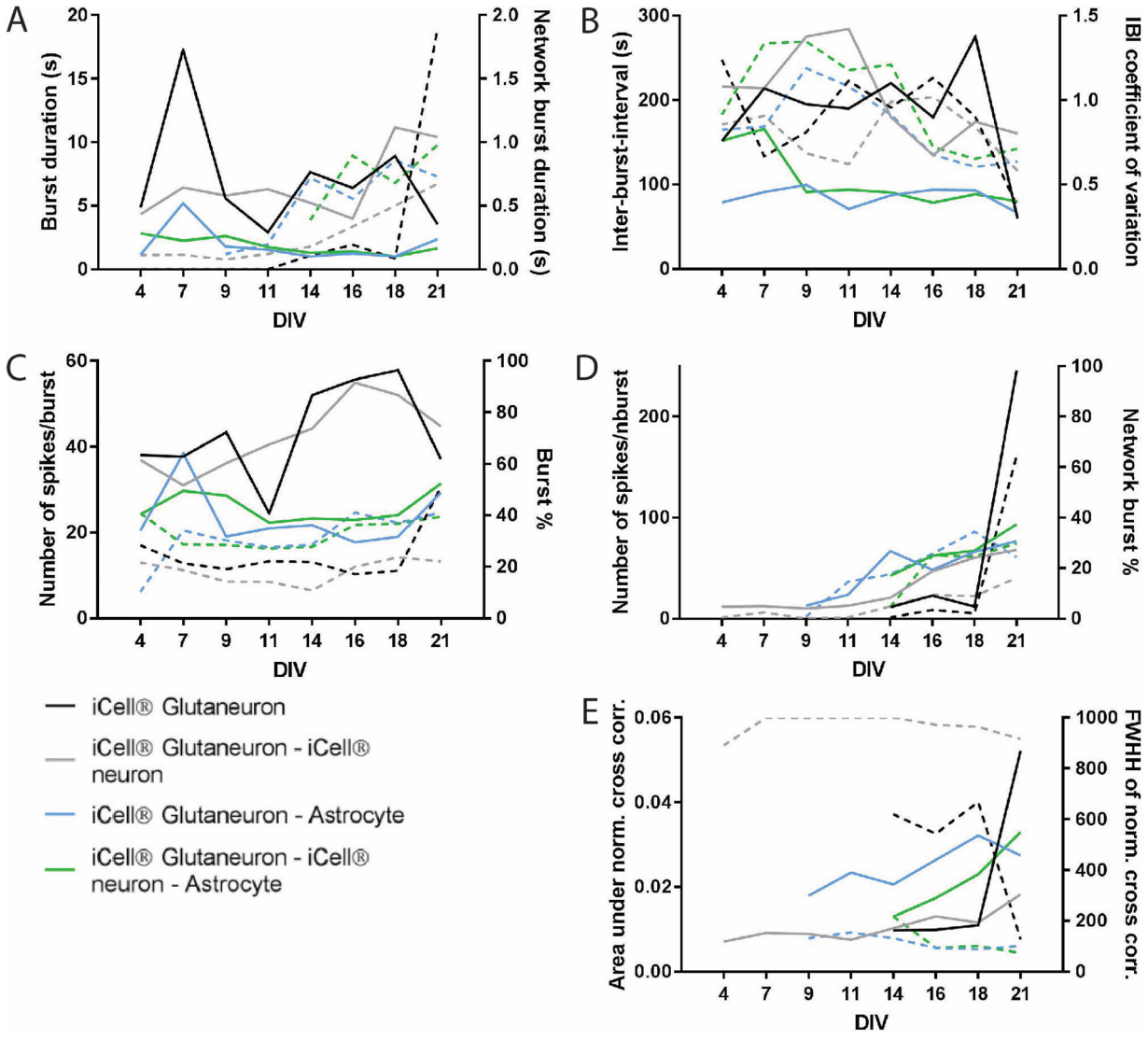


**Fig. 6.** Development of spike and (network) burst activity and synchronicity of the different hiPSC-derived neuronal models. A) Burst duration (s) and network burst duration (s). B) Inter-burst interval (IBI; (s)) and IBI coefficient of variation. C) Number of spikes/burst and percentage of spikes in burst. D) Number of spikes/network burst and percentage of spikes in network burst. E) Area under normalized cross correlation and full width at half height (FWHH). Solid lines match the left y-axis, whereas dashed lines match the right y-axis. Data of the iCell® Glutaneuron monoculture are depicted in black, of the iCell® Glutaneuron-iCell® neuron co-culture in grey, of the iCell® Glutaneuron-Astrocyte co-culture in blue, and of the iCell® Glutaneuron-iCell® neuron-Astrocyte co-culture in green. Data are expressed as mean; for SEM, n and N see Table S1 in the supplemental data. (For interpretation of the references to colour in this figure legend, the reader is referred to the web version of this article).

neurons to iCell® Glutaneurons has limited effect on MSR or the percentage of active wells (Fig. 4A). Similarly, addition of astrocytes to iCell® Glutaneurons or to a co-culture of iCell® Glutaneurons and iCell® neurons (Fig. 5A) has limited effects on spike rates. However, addition of astrocytes does increase the percentage of active wells.

In the absence of astrocytes, the mean burst rate (MBR) is limited and relatively stable over time (Fig. 4B). Addition of astrocytes increases both the MBR and the percentage of bursting wells in a time-dependent manner (Fig. 5B). While the iCell® Glutaneuron-Astrocyte co-culture shows a higher percentage of bursting wells than the iCell® Glutaneuron-iCell® neuron-Astrocyte co-culture, both models show an optimal window for MBR and percentage bursting wells around DIV16-21.

The onset of network bursts also shows some time-dependence, with an increase of the mean network burst rate (MNBR) after 1–2 weeks in culture (Figs. 4C/5C). In the absence of astrocytes, both the MNBR and the percentage of wells with network bursts are limited. Addition of astrocytes to the iCell® Glutaneuron and iCell® Glutaneuron-iCell® neuron co-culture has only a limited effect on MNBR, but clearly increases the percentage of wells with network bursts later in culture, with an optimal window for MBR and percentage bursting wells around DIV16-21 (Fig. 5C).

Further analysis of different parameters for neuronal activity highlights additional differences between our models. Addition of astrocytes decreases burst duration, but increases network burst duration (Fig. 6A). The inter-burst interval (IBI) decreases in the cultures containing astrocytes (Fig. 6B solid line), whereas the IBI coefficient of variation is comparable at the end of culture time for all models (Fig. 6B dashed line). At the peak of the activity of all models (DIV16-18), the number of spikes in a burst is higher in the cultures without astrocytes (Fig. 6C solid line). However, at this time the percentage of spikes that occur in a burst is higher in the astrocyte containing cultures (Fig. 6C dashed line). In regard to the number of spikes per network burst and the percentage of spikes in a network burst, the models behave comparable except for the onset of network bursting (Fig. 6D). Astrocyte containing co-cultures show higher synchrony as indicated by the area

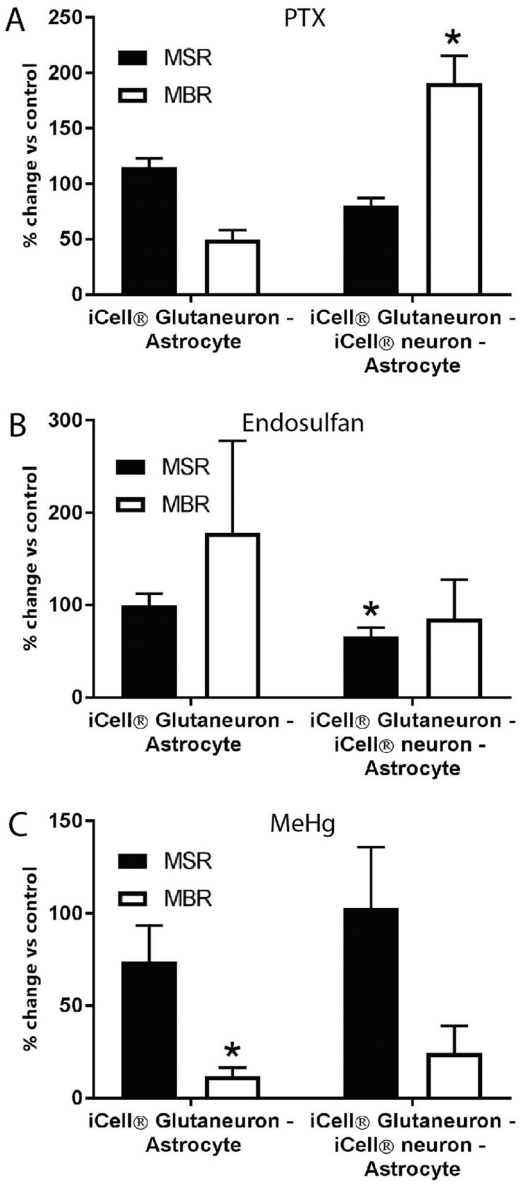


**Fig. 7.** Toxicological modulation of spontaneous activity and bursting of iCell® Glutaneuron-Astrocyte co-culture and iCell® Glutaneuron-iCell® neuron-Astrocyte co-culture. Cultures were exposed at DIV21 to PTX (10 μM; A), endosulfan (1 μM; B) or MeHg (30 μM; C). Data are expressed in MSR or MBR as % of control; mean ± SEM from n = 5–15, N = 4 (A), n = 3–10, N = 2 (B) and n = 3–9, N = 2 (C); * $p < 0.05$.

under normalized cross correlation (Fig. 6E solid line), which is confirmed by the lower full width at half height (FWHH, Fig. 6E dashed line).

### 3.3. Preliminary neurotoxicity assessment

Although all models develop spontaneous neuronal activity and (network) bursting, a culture with astrocytes increase synchronicity (see above), mimics the *in vivo* brain more closely and thus has a clear advantage for neurotoxicity screening. Therefore, we used the neuronal co-cultures with astrocytes for a preliminary neurotoxicity assessment (Fig. 7A–C).

PTX (10 μM), a widely used seizurogenic reference compound, shows limited effects on MSR in both models following acute exposure. However, PTX induces a decrease in MBR in the iCell® Glutaneuron-Astrocyte co-culture, whereas it significantly increases MBR in the iCell® Glutaneuron-iCell® neuron-Astrocyte co-culture (Fig. 7A). The neurotoxic insecticide endosulfan (1 μM), a $GABA_A$ receptor antagonist, has limited effects on the MSR in the iCell® Glutaneuron-Astrocyte co-culture, whereas it increases the MBR of this model. On the other hand, endosulfan exposure significantly reduces MSR in the iCell® Glutaneuron-iCell® neuron-Astrocyte co-culture, but shows no increase in MBR (Fig. 7B). Finally, the known neurotoxicant MeHg (30 μM) has no major effects on MSR for both models (Fig. 7C). MBR is reduced in both models, although significance is reached only for the iCell® Glutaneuron-Astrocyte co-culture.

The difference in chemical sensitivity between the iCell® Glutaneuron-Astrocyte co-culture and the iCell® Glutaneuron-iCell® neuron-Astrocyte co-culture is already apparent from the changes in MSR and MBR. Inclusion of additional metric parameters in a heat map further illustrates these distinctions (Fig. 8).

PTX affects both models differently; where most parameters show a decrease in the iCell® Glutaneuron-Astrocyte co-culture, an increase is visible in the iCell® Glutaneuron-iCell® neuron-Astrocyte co-culture. Similarly, endosulfan changes most of the metric parameters for both co-cultures. Some parameters increase in both models, such as network burst frequency, whereas for most burst-related parameters an opposite effect is seen. Finally, MeHg show a signature that is distinct from those of PTX and endosulfan, although the differences between the two tested co-cultures are less pronounced for MeHg. Overall, these neurotoxicity assessment metrics show that considerable differences exist between both models with respect to chemical sensitivity.

## 4. Discussion

Our immunocytochemistry data demonstrate the homogeneous neuronal nature of the iCell® Glutaneuron monoculture and iCell® Glutaneuron-iCell® co-culture (Fig. 1). Despite the absence of supportive cells, such as astrocytes, these cultures develop into neuronal networks that over time become spontaneously active (Figs. 3 and 4). These cultures already show neuronal activity and bursting as early as DIV4, which remains fairly stable over time (DIV21; Fig. 4A and B). The development of network burst activity, however, shows a time-dependence with an increase after ~2 weeks of culture (Fig. 4C).

Since it is known that astrocytes play an important role in network formation, maturation function (Clarke and Barres, 2013) and protecting neurons from chemical-induced neurotoxicity (Takemoto et al., 2015; Wu et al., 2017), we added astrocytes to our models to more closely resemble the *in vivo* brain. The co-cultures containing astrocytes are more heterogeneous (Fig. 2) and the complexity of the networks increases. Our mwMEA recordings show that co-cultures containing astrocytes, comparable with pure neuronal models, develop spontaneous neuronal activity as early as DIV4, with increased bursting behavior following prolonged culture (DIV14-21; Figs. 3–5). The iCell® Glutaneuron-iCell® neuron-Astrocyte co-culture shows less active bursting wells than the iCell® Glutaneuron-Astrocyte co-culture, although the MSR and MBR are comparable between both cultures (Fig. 5). While the MNBR and the number of spikes in a network burst (Fig. 6D) are comparable between both astrocyte co-culture models, the percentage of wells exhibiting network bursts was highest in the iCell® Glutaneuron-Astrocyte co-culture. Importantly, addition of astrocytes causes our astrocyte co-culture models to fire in a more synchronized manner. This increase in (synchronized) bursting activity by addition of astrocytes is in line with earlier findings (Amiri et al., 2013; Ishii et al., 2017; Kuijlaars et al., 2016). Such synchronized firing is thought to be an important feature for neuronal networks since it is has been suggested to be involved in cognitive and sensory processes (Engel et al., 2001; Ward, 2003). Overall, both our astrocyte co-cultures show a development comparable to that described for rat primary cortical neurons (Brown et al., 2016), with increasing MSR, MBR and number of spikes in network bursts during development (Figs. 5 and 6).

As the two astrocyte co-culture models show a stable MSR, with a

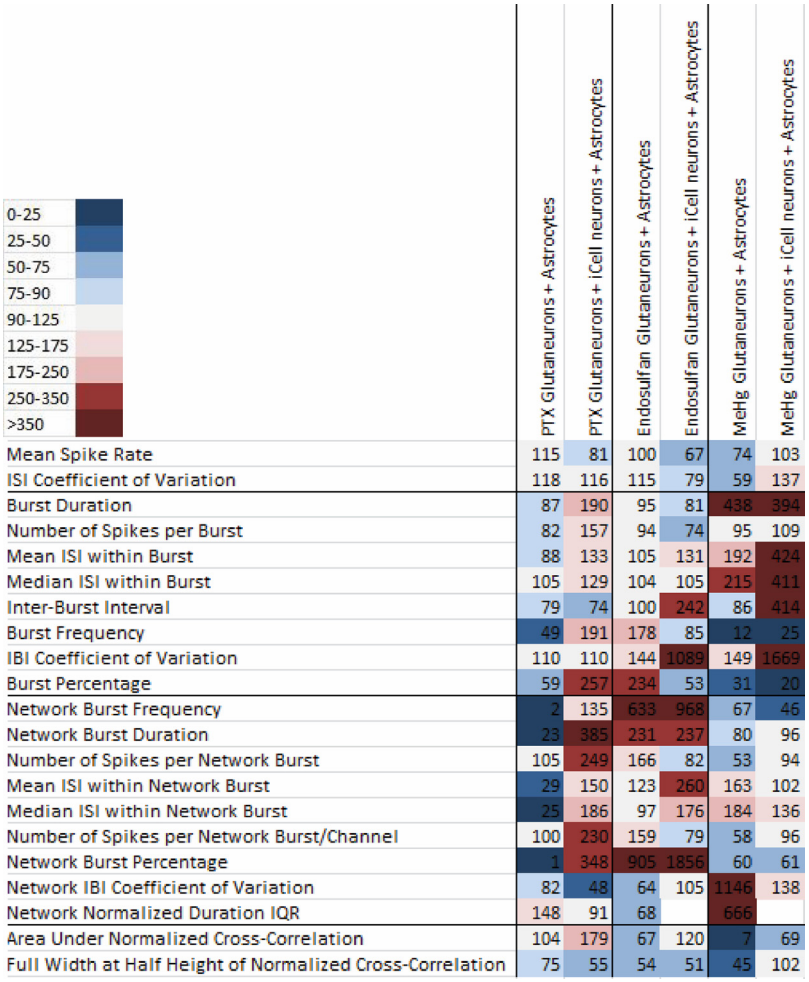


| | PTX Glutaneurons + Astrocytes | PTX Glutaneurons + iCell neurons + Astrocytes | Endosulfan Glutaneurons + Astrocytes | Endosulfan Glutaneurons + iCell neurons + Astrocytes | MeHg Glutaneurons + Astrocytes | MeHg Glutaneurons + iCell neurons + Astrocytes |
|---|---|---|---|---|---|---|
| Mean Spike Rate | 115 | 81 | 100 | 67 | 74 | 103 |
| ISI Coefficient of Variation | 118 | 116 | 115 | 79 | 59 | 137 |
| Burst Duration | 87 | 190 | 95 | 81 | 438 | 394 |
| Number of Spikes per Burst | 82 | 157 | 94 | 74 | 95 | 109 |
| Mean ISI within Burst | 88 | 133 | 105 | 131 | 192 | 424 |
| Median ISI within Burst | 105 | 129 | 104 | 105 | 215 | 411 |
| Inter-Burst Interval | 79 | 74 | 100 | 242 | 86 | 414 |
| Burst Frequency | 49 | 191 | 178 | 85 | 12 | 25 |
| IBI Coefficient of Variation | 110 | 110 | 144 | 1089 | 149 | 1669 |
| Burst Percentage | 59 | 257 | 234 | 53 | 31 | 20 |
| Network Burst Frequency | 2 | 135 | 633 | 968 | 67 | 46 |
| Network Burst Duration | 23 | 385 | 231 | 237 | 80 | 96 |
| Number of Spikes per Network Burst | 105 | 249 | 166 | 82 | 53 | 94 |
| Mean ISI within Network Burst | 29 | 150 | 123 | 260 | 163 | 102 |
| Median ISI within Network Burst | 25 | 186 | 97 | 176 | 184 | 136 |
| Number of Spikes per Network Burst/Channel | 100 | 230 | 159 | 79 | 58 | 96 |
| Network Burst Percentage | 1 | 348 | 905 | 1856 | 60 | 61 |
| Network IBI Coefficient of Variation | 82 | 48 | 64 | 105 | 1146 | 138 |
| Network Normalized Duration IQR | 148 | 91 | 68 | | 666 | |
| Area Under Normalized Cross-Correlation | 104 | 179 | 67 | 120 | 7 | 69 |
| Full Width at Half Height of Normalized Cross-Correlation | 75 | 55 | 54 | 51 | 45 | 102 |

**Fig. 8.** Heat map of the effects of PTX, endosulfan and MeHg on selected metric parameters on iCell® Glutaneuron-Astrocyte co-cultures and iCell® Glutaneuron-iCell® neuron-Astrocyte co-cultures. Values in cells are means, expressed as % of control from n = 3–15; N = 2-4. Color scaling is based on the magnitude of the % of change relative to control. For empty cells no average could be calculated.

clear optimum for bursting activity, network burst activity and synchronized firing at DIV14-21, we used these two models to perform a preliminary neurotoxicity assessment at DIV21. Because we want our models to be able to detect seizures we choose two compounds for our preliminary neurotoxicity assessment that reportedly increase neuronal activity: PTX and endosulfan. The seizurogenic GABA receptor antagonists PTX causes an concentration-dependent increase in MSR in rat primary cortical cultures (Mack et al., 2014; Tukker et al., unpublished). However, exposure of the iCell® Glutaneuron-Astrocyte co-culture to PTX was without major effects on MSR and MBR (Fig. 7). Similarly, exposure of the iCell® Glutaneuron-Astrocyte co-culture to endosulfan is without major effects on MSR and MBR, whereas it causes a profound increase in MSR in rat primary cortical cultures (Dingemans et al., 2016). This apparent lack of chemosensitivity of the iCell® Glutaneuron-Astrocyte co-culture could be a result of the high fraction of excitatory neurons, which results in a relatively high MSR and MBR that is not easily increased further following exposure to seizurogenic compounds. Alternatively, the apparent lack of chemosensitivity in the iCell® Glutaneuron-Astrocyte co-culture could be a direct result of the sparsity of GABAergic receptors, which may act as a specific target for PTX and endosulfan.

In line with these suggestions, the iCell® Glutaneuron-iCell® neuron-Astrocyte co-culture has a lower MBR than the iCell® Glutaneuron-Astrocyte co-culture, which is likely due to the larger fraction of inhibitory GABAergic neurons. Notably, exposure of the iCell® Glutaneuron-iCell® neuron-Astrocyte co-culture to PTX does result in an apparent increase in MBR, but without effect on MSR. Endosulfan lowers MSR, without affecting the MBR. These findings suggest that the effects of PTX and endosulfan may be distinguished by taking other metric parameters into account. Our heat map (Fig. 8) shows that indeed other parameters such as burst percentage, network burst duration and network burst percentage are affected in a stronger manner. Importantly, the chemosensitivity towards GABA receptor antagonists or seizurogenic compounds in general may thus critically depend on the fraction of inhibitory neurons in the network and/or the degree of excitability prior to exposure. This would also explain some of the discrepancies reported earlier, *e.g.* Kuijlaars et al. (2016) report a decrease in bursting frequency on their iPSC-derived model following exposure to PTX.

While the iCell® Glutaneuron-iCell® neuron-Astrocyte co-culture is more sensitive to PTX and endosulfan than the iCell® Glutaneuron-Astrocyte co-culture, the latter is more responsive to MeHg. In rat primary cortical cultures, exposure to MeHg results in a profound decrease of MSR (Dingemans et al., 2016). At the concentrations chosen and limited exposure time (30 min) it is unlikely that the reported effects are confounded by acute cytotoxicity. This notion is further strengthened by the absence of cytotoxicity in rat primary cortical cultures (Dingemans et al., 2016; Tukker et al., unpublished; Yuan and Atchison, 2007; Yuan et al., 2005). Exposure of the iCell® Glutaneuron-Astrocyte co-culture to MeHg also causes a clear decrease in MBR, but is without effect in the iCell® Glutaneuron-iCell® neuron-Astrocyte co-culture. Since MeHg is expected to decrease neuronal activity, it is possible that

culture models with a relatively high MSR and MBR are more sensitive towards neurotoxicants that reduce activity, contrary to the chemosensitivity towards seizurogenic compounds which seems to be higher in cultures with less excitation.

When the toxicity heat map data reported here (Fig. 8) is compared to published primary rat cortical data, we find that our iCell® Glutaneuron-Astrocyte co-culture exposed to PTX exhibits a similar pattern (Bradley et al., 2018). Network burst duration, number of spikes per network burst, and burst duration all show an increase as compared to control, whereas the full width at half height shows a decrease. The PTX heat map of our iCell Glutaneuron–iCell neuron–Astrocyte co-culture model also matches with Bradley et al. (2018). Number of spikes per burst and median burst duration both show a decrease and the inter burst interval shows a decrease. However, the heat map pattern is clearly concentration-dependent (Bradley et al., 2018), which may also explain why our endosulfan heat map does not match their pattern.

In conclusion, we show that the commercially available hiPSC-derived models investigated in this study all form neuronal networks consisting of inhibitory GABAergic and excitatory glutamatergic neurons. These networks develop spontaneous neuronal activity and bursting. Addition of astrocytes to the cultures changes the activity pattern resulting in synchronized activity of the network. Despite the limited test set of compounds, our data already show that these models exert different responses following exposure to seizurogenic compounds and neurotoxicants. Our preliminary neurotoxicity assessment indicates that the sensitivity of hiPSC-derived neuronal models depends on the ratio of GABAergic and glutamatergic neurons, either because this affects the intrinsic degree of neuronal activity (MSR/MBR) or because it changes the degree of available target cells (GABA/glutamate receptors). Further characterization and toxicological validation of the different co-cultures models available are thus urgently needed. While currently hampered by the expense of hiPSCs, such validation should involve a more extensive set of reference compounds (including additional positive and negative controls that cover different modes of action) at multiple concentrations. Nevertheless, our preliminary data already provide a proof-of-principle for the usability of hiPSC-derived neuronal co-culture models for neurotoxicological screening in the mwMEA. A breakthrough of these hiPSC-derived neuronal models may enable animal-free neurotoxicity testing in the future, but may at present already be used as a prioritization tool prior to *in vivo* studies.

## Conflict of interest

The authors declare that there are no conflicts of interest. Given his role as Editor in Chief of NeuroToxicology, Remco H.S. Westerink had no involvement in the peer-review of this article and has no access to information regarding its peer-review. Full responsibility for the editorial process for this article was delegated to Pamela J. Lein.

## Acknowledgements

Members of the Neurotoxicology Research Group, Mimetas (Leiden, The Netherlands), Cellular Dynamics International (Madison, WI, USA) and the NC3R team are gratefully acknowledged for helpful discussions. This work was funded by a grant from the National Centre for the Replacement, Refinement and Reduction of Animals in Research (NC3Rs; project number 50308-372160), the Netherlands Organisation for Health Research and Development (ZonMW; InnoSysTox project number 114027001) and by the Faculty of Veterinary Medicine (Utrecht University, The Netherlands).

## Appendix A. Supplementary data

Supplementary material related to this article can be found, in the online version, at doi: https://doi.org/10.1016/j.neuro.2018.06.007.

## References

Alloisio, S., Nobile, M., Novellino, A., 2015. Multiparametric characterisation of neuronal network activity for in vitro agrochemical neurotoxicity assessment. Neurotoxicology 48, 152–165. http://dx.doi.org/10.1016/j.neuro.2015.03.013.

Amiri, M., Hosseinmardi, N., Bahrami, F., Janahmadi, M., 2013. Astrocyte- neuron interaction as a mechanism responsible for generation of neural synchrony: a study based on modeling and experiments. J. Comput. Neurosci. 34, 489–504. http://dx.doi.org/10.1007/s10827-012-0432-6.

Anson, B.D., Kolaja, K.L., Kamp, T.J., 2011. Opportunities for use of human iPS cells in predictive toxicology. Clin. Pharmacol. Ther. 89, 754–758. http://dx.doi.org/10.1038/clpt.2011.9.

Bradley, S., Luithardt, H.H., Metea, M.R., Strock, C.J., 2018. *In vitro* screening for seizure liability using microelectrode array technology. Toxicol. Sci. 1–14. http://dx.doi.org/10.1093/toxsci/kfy029.

Brown, J.P., Hall, D., Frank, C.L., Wallace, K., Mundy, W.R., Shafer, T.J., 2016. Evaluation of a microelectrode array-based assay for neural network ontogeny using training set chemicals. Toxicol. Sci. 154, 126–139. http://dx.doi.org/10.1093/toxsci/kfw147.

Clarke, L.E., Barres, B.A., 2013. Emerging roles of astrocytes in neural circuit development. Nat. Rev. Neurosci. 14 (5), 311–321. http://dx.doi.org/10.1038/nrn3484.

de Groot, M.W.G.D.M., Dingemans, M.M.L., Rus, K.H., de Groot, A., Westerink, R.H.S., 2014. Characterization of calcium responses and electrical activity in differentiating mouse neural progenitor cells in vitro. Toxicol. Sci. 137, 428–435. http://dx.doi.org/10.1093/toxsci/kft261.

Dingemans, M.M.L., Schütte, M.G., Wiersma, D.M.M., de Groot, A., van Kleef, R.G.D.M., Wijnolts, F.M.J., Westerink, R.H.S., 2016. Chronic 14-day exposure to insecticides or methylmercury modulates neuronal activity in primary rat cortical cultures. Neurotoxicology 57, 194–202. http://dx.doi.org/10.1016/j.neuro.2016.10.002.

Engel, A.K., Fries, P., Singer, W., 2001. Dynamic predictions: oscillations and synchrony in top–down processing. Nat. Rev. Neurosci. 2, 704–716. http://dx.doi.org/10.1038/35094565.

Görtz, P., Fleischer, W., Rosenbaum, C., Otto, F., Siebler, M., 2004. Neuronal network properties of human teratocarcinoma cell line-derived neurons. Brain Res. 1018, 18–25. http://dx.doi.org/10.1016/j.brainres.2004.05.076.

Hartung, T., 2008. Thoughts on limitations of animal models. Parkinsonism Relat. Disord. 14. http://dx.doi.org/10.1016/j.parkreldis.2008.04.003.

Hogberg, H.T., Sobanski, T., Novellino, A., Whelan, M., Weiss, D.G., Bal-Price, A.K., 2011. Application of micro-electrode arrays (MEAs) as an emerging technology for developmental neurotoxicity: evaluation of domoic acid-induced effects in primary cultures of rat cortical neurons. Neurotoxicology 32, 158–168. http://dx.doi.org/10.1016/j.neuro.2010.10.007.

Hondebrink, L., Verboven, A.H.A., Drega, W.S., Schmeink, S., De Groot, M.W.G.D.M., Van Kleef, R.G.D.M., Wijnolts, F.M.J., De Groot, A., Meulenbelt, J., Westerink, R.H.S., 2016. Neurotoxicity screening of (illicit) drugs using novel methods for analysis of microelectrode array (MEA) recordings. Neurotoxicology 55, 1–9. http://dx.doi.org/10.1016/j.neuro.2016.04.020.

Hyysalo, A., Ristola, M., Mäkinen, M.E.L., Häyrynen, S., Nykter, M., Narkilahti, S., 2017. Laminin α5 substrates promote survival, network formation and functional development of human pluripotent stem cell-derived neurons in vitro. Stem Cell Res. 24, 118–127. http://dx.doi.org/10.1016/j.scr.2017.09.002.

Ishii, M.N., Yamamoto, K., Shoji, M., Asami, A., Kawamata, Y., 2017. Human induced pluripotent stem cell (hiPSC)-derived neurons respond to convulsant drugs when co-cultured with hiPSC-derived astrocytes. Toxicology 389, 130–138. http://dx.doi.org/10.1016/j.tox.2017.06.010.

Kuijlaars, J., Oyelami, T., Diels, A., Rohrbacher, J., Versweyveld, S., Meneghello, G., Tuefferd, M., Verstraelen, P., Detrez, J.R., Verschuuren, M., De Vos, W.H., Meert, T., Peeters, P.J., Cik, M., Nuydens, R., Brône, B., Verheyen, A., 2016. Sustained synchronized neuronal network activity in a human astrocyte co-culture system. Sci. Rep. 6. http://dx.doi.org/10.1038/srep36529.

Legéndy, C.R., Salcman, M., 1985. Bursts and recurrences of bursts in the spike trains of spontaneously active striate cortex neurons. J. Neurophysiol. 53, 926–939. http://dx.doi.org/10.1152/jn.1985.53.4.926.

Mack, C.M., Lin, B.J., Turner, J.D., Johnstone, A.F.M., Burgoon, L.D., Shafer, T.J., 2014. Burst and principal components analyses of MEA data for 16 chemicals describe at least three effects classes. Neurotoxicology 40, 75–85. http://dx.doi.org/10.1016/j.neuro.2013.11.008.

McConnell, E.R., McClain, M.A., Ross, J., LeFew, W.R., Shafer, T.J., 2012. Evaluation of multi-well microelectrode arrays for neurotoxicity screening using a chemical training set. Neurotoxicology 33, 1048–1057. http://dx.doi.org/10.1016/j.neuro.2012.05.001.

Meneghello, G., Verheyen, A., Van Ingen, M., Kuijlaars, J., Tuefferd, M., Van Den Wyngaert, I., Nuydens, R., 2015. Evaluation of established human iPSC-derived neurons to model neurodegenerative diseases. Neuroscience 301, 204–212. http://dx.doi.org/10.1016/j.neuroscience.2015.05.071.

Nicolas, J., Hendriksen, P.J.M., van Kleef, R.G.D.M., de Groot, A., Bovee, T.F.H., Rietjens, I.M.C.M., Westerink, R.H.S., 2014. Detection of marine neurotoxins in food safety testing using a multielectrode array. Mol. Nutr. Food Res. 58, 2369–2378. http://dx.doi.org/10.1002/mnfr.201400479.

Odawara, A., Katoh, H., Matsuda, N., Suzuki, I., 2016. Physiological maturation and drug responses of human induced pluripotent stem cell-derived cortical neuronal networks in long-term culture. Sci. Rep. 6. http://dx.doi.org/10.1038/srep26181.

Paavilainen, T., Pelkonen, A., Mäkinen, M.E.-L., Peltola, M., Huhtala, H., Fayuk, D., Narkilahti, S., 2018. Effect of prolonged differentiation on functional maturation of human pluripotent stem cell-derived neuronal cultures. Stem Cell Res. 27. http://dx.

doi.org/10.1016/j.scr.2018.01.018.
Pamies, D., Hartung, T., 2017. 21st century cell culture for 21st century toxicology. Chem. Res. Toxicol. 30, 43–52. http://dx.doi.org/10.1021/acs.chemrestox.6b00269.
Pleil, J.D., 2016. Comparing biomarker measurements to a normal range: when to use standard error of the mean (SEM) or standard deviation (SD) confidence intervals tests. Biomarkers 21 (3), 195–199. http://dx.doi.org/10.3109/1354750X.2015.1134666.
Strickland, J.D., LeFew, W.R., Crooks, J., Hall, D., Ortenzio, J.N., Dreher, K., Shafer, T.J., 2016. In vitro screening of metal oxide nanoparticles for effects on neural function using cortical networks on microelectrode arrays. Nanotoxicology 10, 619–628. http://dx.doi.org/10.3109/17435390.2015.1107142.
Takemoto, T., Ishihara, Y., Ishida, A., Yamazaki, T., 2015. Neuroprotection elicited by nerve growth factor and brain-derived neurotrophic factor released from astrocytes in response to methylmercury. Environ. Toxicol. Pharmacol. 40, 199–205. http://dx.doi.org/10.1016/j.etap.2015.06.010.
Tang, X., Zhou, L., Wagner, A.M., Marchetto, M.C.N., Muotri, A.R., Gage, F.H., Chen, G., 2013. Astroglial cells regulate the developmental timeline of human neurons differentiated from induced pluripotent stem cells. Stem Cell. Res. 11, 743–757. http://dx.doi.org/10.1016/j.scr.2013.05.002.
Tukker, A.M., De Groot, M.W.G.D.M., Wijnolts, F.M.J., Kasteel, E.E.J., Hondebrink, L., Westerink, R.H.S., 2016. Research article is the time right for in vitro neurotoxicity testing using human iPSC-derived neurons? ALTEX 33, 261–271. http://dx.doi.org/10.14573/altex.1510091.
Valdivia, P., Martin, M., LeFew, W.R., Ross, J., Houck, K.A., Shafer, T.J., 2014. Multi-well microelectrode array recordings detect neuroactivity of ToxCast compounds. Neurotoxicology 44, 204–217. http://dx.doi.org/10.1016/j.neuro.2014.06.012.
Vassallo, A., Chiappalone, M., De Camargos Lopes, R., Scelfo, B., Novellino, A., Defranchi, E., Palosaari, T., Weisschu, T., Ramirez, T., Martinoia, S., Johnstone, A.F.M., Mack, C.M., Landsiedel, R., Whelan, M., Bal-Price, A., Shafer, T.J., 2017. A multi-laboratory evaluation of microelectrode array-based measurements of neural network activity for acute neurotoxicity testing. Neurotoxicology 60, 280–292. http://dx.doi.org/10.1016/j.neuro.2016.03.019.
Ward, L.M., 2003. Synchronous neural oscillations and cognitive processes. Trends Cogn. Sci. 7 (12), 553–559. http://dx.doi.org/10.1016/j.tics.2003.10.012.
Westerink, R.H.S., 2013. Do we really want to REACH out to in vitro? Neurotoxicology 39, 169–172. http://dx.doi.org/10.1016/j.neuro.2013.10.001.
Wu, X., Yang, X., Majumder, A., Swetenburg, R., Goodfellow, F.T., Bartlett, M.G., Stice, S.L., 2017. Astrocytes are protective against chlorpyrifos developmental neurotoxicity in human pluripotent stem cell-derived astrocyte-neuron cocultures. Toxicol. Sci. 157, 410–420. http://dx.doi.org/10.1093/toxsci/kfx056.
Yuan, Y., Atchison, W.D., 2007. Methylmercury-induced increase of intracellular Ca2+ increases spontaneous synaptic current frequency in rat cerebellar slices. Mol. Pharmacol. 71, 1109–1121. http://dx.doi.org/10.1124/mol.106.031286.both.
Yuan, Y., Otero-Montañez, J.K.L., Yao, A., Herden, C.J., Sirois, J.E., Atchison, W.D., 2005. Inwardly rectifying and voltage-gated outward potassium channels exhibit low sensitivity to methylmercury. Neurotoxicology 26, 439–454. http://dx.doi.org/10.1016/j.neuro.2005.03.005.